

Activation enthalpy, Gibbs free energy, and entropy for conduction in Na β'' -alumina

J. C. Wang

Solid State Division, Oak Ridge National Laboratory, Oak Ridge, Tennessee 37830

(Received 14 June 1982)

The temperature-dependent activation enthalpy ΔH , Gibbs free energy ΔG , and entropy ΔS for the vacancy conduction in Na β'' -alumina were extracted from the conductivity data. The value of ΔH calculated from the equation $\Delta H = -d \ln(\sigma T) / d(1/kT)$ decreases from ~ 0.3 eV at low T to ~ 0.03 eV at high T in a form that can be correlated to the decrease of vacancy ordering on a superlattice reported from diffuse x-ray scattering studies. This T variation in ΔH requires a T variation in ΔS according to the thermodynamic relation $d\Delta S/dT = (1/T)d\Delta H/dT$. By setting the integration constant to be zero, the value of ΔS was found to decrease from $\sim 7k$ (10^{-22} J/K) at low T to ~ 0 at high T . As a result, the activation free energy $\Delta G = \Delta H - T\Delta S$ is much smaller than ΔH at low T . The results are consistent with the calculated small activation energy for diffusion of a single vacancy (~ 0.02 eV) and the assignment of a low-frequency (~ 30 cm^{-1}) Raman peak to the attempt mode for diffusion.

I. INTRODUCTION

The β'' -aluminas, like β -aluminas, constitute a family of solid electrolytes in which the ionic conduction is two dimensional within the conduction layers which are separated by closely packed spinel blocks.¹ However, unlike β -aluminas, the $\log(\sigma T)$ vs $1/T$ plots for the β'' -aluminas show an unusual non-Arrhenius behavior: The absolute values of their slopes are high at low temperatures and decrease gradually with increasing temperature (Fig. 1).²⁻⁶ It has been suggested that this non-Arrhenius behavior may originate from the change with temperature of conducting-cation ordering on a superlattice.⁷⁻⁹ A comparison of conductivity and diffuse x-ray scattering measurements indicates that higher activation energies are associated with greater ordering of conducting cations on the superlattice.¹⁰ In this work, we present a theoretical model which connects the temperature dependence of the activation energy with the change in superlattice ordering.

Sato and Kikuchi^{11,12} have treated the β'' -alumina problem with the cluster variation and the path probability methods using a two-dimensional honeycomb network. Their results show that the conductivity is non-Arrhenius for some conducting-cation concentrations. However, because they used only a nearest-neighbor interaction potential between the cations, their results are not suitable to describe the long-range ordering of the cation on the superlattice. An actual application¹³ to Na β'' -alumina using the experimentally deter-

mined Na^+ concentration indicates that these methods cannot explain the non-Arrhenius behavior of the material with the present interaction potential.

Usually results of conductivity measurements for ionic crystals are presented as graphs of $\log(\sigma T)$ vs $1/T$. For a crystal having a linear Arrhenius plot

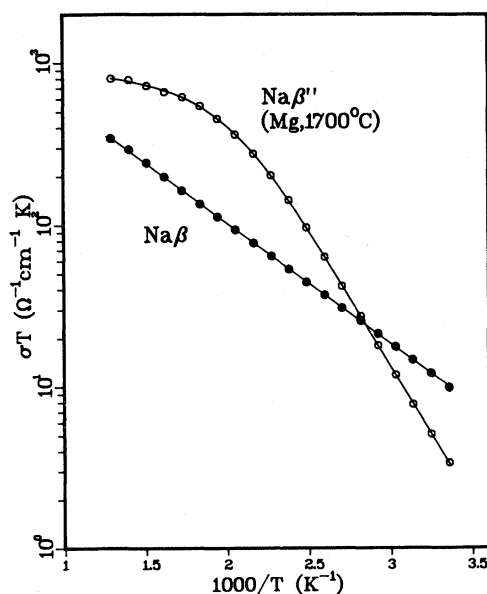


FIG. 1. Conductivity Arrhenius plots for Na β - and β'' -alumina taken from Refs. 14 and 6, respectively. The Na β'' sample was grown at 1700°C and stabilized with magnesium. The solid lines are smooth curves used in this work to represent the experimental data.

such as that of Na β -alumina taken from Ref. 14 and shown in Fig. 1, the slope of the graph determines the activation enthalpy for conduction. However, for a crystal with a nonlinear Arrhenius plot such as that of Na β'' -alumina (Fig. 1), the slope of the curve is temperature dependent, and its meaning is unclear. For example, if the curvature of an Arrhenius plot is caused by the presence of two simultaneous conduction processes with different constant activation enthalpies:

$$\sigma T = \sigma_{01} e^{-\Delta H_1/kT} + \sigma_{02} e^{-\Delta H_2/kT}, \quad (1)$$

then the slope of the $\log(\sigma T)$ vs $1/T$ curve determines neither of the activation enthalpies. It is interesting to note that the curvature caused by the presence of two simultaneous conduction processes, Eq. (1), is always of the opposite sense to that shown in Fig. 1 and can never account for the experimentally observed curvature.

In this work, we first extract the activation enthalpy, entropy, and Gibbs free energy for conduction in Na β'' -alumina from the conductivity data. Then, by interpreting the results, we discuss the conduction mechanism for the material.

II. CALCULATION METHOD

As shown in Ref. 15 and also in the Appendix, if a $\log(\sigma T)$ vs $1/T$ plot is continuous and smooth, it is always possible to express σT as

$$\sigma T = \nu_0 C \exp\{-[\Delta H(T) - T\Delta S(T)]/kT\}, \quad (2)$$

where the product $\nu_0 C$ is a constant and where the functions $\Delta H(T)$ and $\Delta S(T)$ satisfy the relation

$$\frac{d\Delta H(T)}{dT} = \frac{Td\Delta S(T)}{dT}. \quad (3)$$

It should be emphasized here that Eqs. (2) and (3) are obtained from geometric consideration alone (see the Appendix); so far no physical meaning has been associated with the functions $\Delta H(T)$ and $\Delta S(T)$.

In this work we assume that the conductivity of Na β'' -alumina arises from a single mechanism (vacancy mechanism) in the thermally activated form:

$$\sigma T = \nu_0 C e^{-\Delta G(T)/kT}, \quad (4)$$

where ν_0 is the attempt frequency along a given direction, C is a constant determined by the

conducting-cation concentration and the geometry of the crystal, and $\Delta G(T)$ is the temperature-dependent activation Gibbs free energy for the mechanism and is related to the activation enthalpy $\Delta H(T)$ and entropy $\Delta S(T)$ by the thermodynamic relation

$$\Delta G(T) = \Delta H(T) - T\Delta S(T). \quad (5)$$

By making this assumption, situations such as that described by Eq. (1) are excluded from our consideration. It is this assumption that enables us to identify the functions $\Delta H(T)$ and $\Delta S(T)$ in Eqs. (2) and (3) with the activation enthalpy and entropy,¹⁵ respectively, which appear in Eq. (5). Notice that the relation between the functions $\Delta H(T)$ and $\Delta S(T)$, Eq. (3), is consistent with the thermodynamic relation between the enthalpy and entropy under constant pressure.

The experimental heat of activation (or apparent activation energy) is defined from the slope of a $\log(\sigma T)$ vs $1/T$ plot as

$$Q(T) = \frac{-d[\ln(\sigma T)]}{d(1/kT)}. \quad (6)$$

By differentiating Eq. (2) and using Eq. (3), it follows that

$$Q(T) = \Delta H(T), \quad (7)$$

i.e., the experimental heat of activation obtained from the slope of the Arrhenius plot is identical to the activation enthalpy under our single-mechanism assumption.

The procedure for calculating ΔH , ΔS , and ΔG for conduction is summarized as follows:

(i) Calculate $\Delta H(T)$ from the slope of the experimental $\log(\sigma T)$ vs $1/T$ plot with Eqs. (6) and (7).

(ii) Calculate the $\Delta S(T)$ by integrating Eq. (3) and using the result of (i).

(iii) Calculate $\Delta G(T)$ with Eq. (5).

III. RESULTS

To extract the activation enthalpy from the experimental conductivity data for Na β'' -alumina with Eqs. (6) and (7), we need first to find a smooth curve to represent the data so that we can calculate the slope of the Arrhenius plot. There is no unique way to accomplish this. In our case, we tried various functions which give constant $\Delta H(T)$ at small T and give decreasing $\Delta H(T)$ with increasing T . A good fit was obtained by using the function

$$\sigma T = \begin{cases} \nu_0 C \exp\{-[E_0 - E_1 \tanh(T/T_0 - T_1/T_0)]/kT\}, & T \geq T_1 \\ \nu_0 C \exp\{-[E_0 - E_1(T/T_0 - T_1/T_0)]/kT\}, & T < T_1 \end{cases} \quad (8)$$

where $\nu_0 C$, E_0 , E_1 , T_0 , and T_1 are fitting parameters. The result for the conductivity data taken from Ref. 6 is shown in Fig. 1. Notice that here we are only interested in finding a smooth curve to represent the data; the arbitrariness in the procedure used should not change the main results of our analysis. By differentiating the curve with respect to $(1/kT)$, one gets the activation enthalpy of conduction, $\Delta H(T)$. The result is shown by the solid line in Fig. 2.

To calculate the activation entropy from $\Delta H(T)$, we integrate Eq. (3) to get

$$\Delta S(T) = \Delta H(T)/T + \int_T dx \Delta H(x)/x^2 + \Delta S_0, \quad (9)$$

where ΔS_0 is an integration constant. We set $\Delta S_0 = 0$ [i.e., $\Delta S(T) = 0$ at $T = \infty$] because, as shown later, this leads to a reasonable value of the attempt frequency ν_0 . The calculated activation entropy for the conductivity curve of Na β'' -alumina in Fig. 1 is shown by the dashed line in Fig. 2. The corresponding activation Gibbs free energy calculated with Eq. (5) is also shown in the same figure.

IV. DISCUSSION

A. Temperature dependence of ΔH

As shown in Fig. 2, the activation enthalpy $\Delta H(T)$ has a constant value of about 0.33 eV below 350 K and decreases with increasing temperature to about 0.03 eV at 750 K. An interesting question is what is the origin of this drastic change in activation enthalpy with temperature. To answer this question, we first review briefly the structure of β'' -alumina.

The conduction layer of Na β'' -alumina consists of bridging oxygen ions O(5), which separate the closely packed spinel blocks,¹ and conducting Na⁺ ions which occupy tetrahedral sites formed by the oxygen ions [O(2) and O(4)] of the spinel blocks. The Na⁺ sites are slightly shifted from the plane formed by O(5) ions and are only partially occupied ($\sim \frac{5}{6}$).^{8,16} Figure 3 shows schematically the structure of this conduction layer. In the figure, $\frac{1}{6}$ of the Na⁺ sites are vacant and are arranged on a superlattice according to the results reported from diffuse x-ray scattering studies.^{7,8} The projection of the lines connecting neighboring Na⁺ sites on the O(5) plane forms a two-dimensional honeycomb conduction network. A possible model for analyzing the conductivity of Na⁺ β'' -alumina is to treat

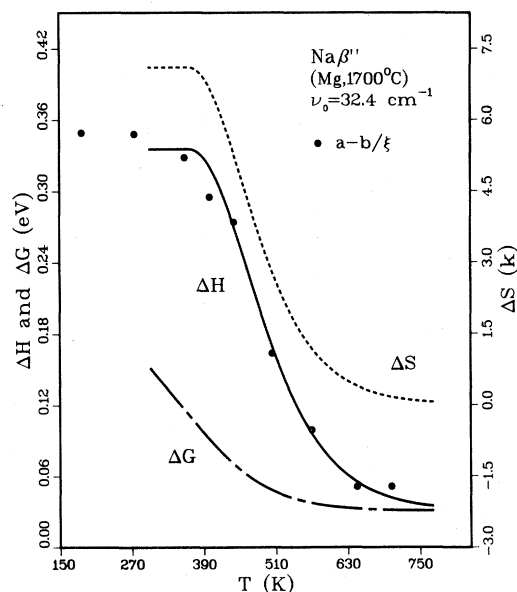


FIG. 2. Activation enthalpy (ΔH), entropy (ΔS), and Gibbs free energy (ΔG) for conduction calculated from the conductivity data of Na β'' in Fig. 1. The dots show the two-parameter least-squares fit of the activation enthalpy with $\Delta H(T) = a - b/\xi(T)$, where $\xi(T)$ is the experimental coherence length of the superlattice determined by diffuse x-ray scattering and taken from Ref. 8.

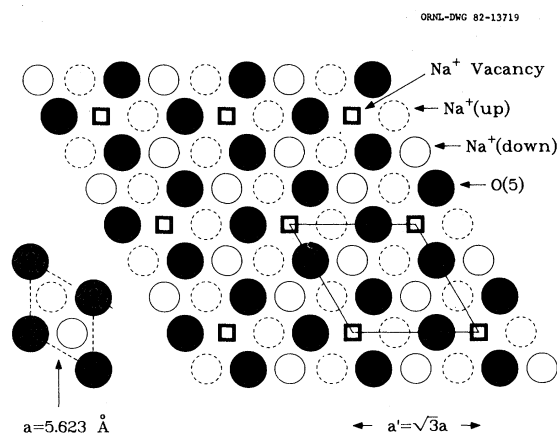


FIG. 3. Schematic diagram of a superlattice structure of vacancies (squares) in the conduction layer of Na β'' with $\frac{1}{6}$ of the Na⁺ sites vacant. The dashed circles represent one-half of the Na⁺ sites which are about 0.16 Å above the plane formed by the bridging oxygen ions [O(5)]. The vacancies and other Na⁺ sites (solid circles) are about 0.16 Å below the plane. The planar lattice parameter of the superlattice (a') is $\sqrt{3}$ times that of the regular lattice (a).

the vacancies as quasiparticles jumping on the conduction network. The vacancies and the network are shown in Fig. 4.

Potential-energy calculations^{17,18} using Coulomb, core-repulsive, and polarization terms have been made for a single Na^+ vacancy in the ideal structure of $\text{Na } \beta''\text{-alumina}$. All but one of the Na^+ sites were assumed to be occupied [Fig. 4(b)]. The potential barrier height for the vacancy to jump to a neighboring site was found to be extremely low (~ 0.02 eV), i.e., the vacancy is "nearly free" in this case. This result can be understood by considering the following: Let us assume that the host lattice provides N potential wells with depth V_0 , and that there are $N-1$ Na^+ ions, i.e., there is only one vacancy. If we first assume that the Na^+ ions do not interact with one another, then the barrier height for a Na^+ ion next to the vacancy to jump into it is exactly V_0 . If now the repulsive potential between Na^+ ions is turned on, the barrier height for the Na^+ ion to jump is reduced to a value smaller than V_0 because it receives no repulsion from the vacancy. It was demonstrated in a one-dimensional model study¹⁹ that when the repulsive interaction is strong enough, the activation energy for vacancy conduction can become very small. A similar conclusion was also reached when the path probability method of Sato and Kikuchi^{11,12} was applied to the $\text{Na } \beta''\text{-alumina}$ problem.¹³

The result that the calculated activation energy for a single vacancy to jump is small (~ 0.02 eV) is consistent with the low activation enthalpy ΔH at

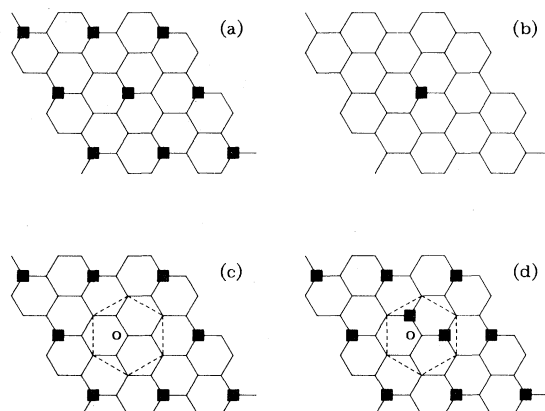


FIG. 4. Schematic diagrams of vacancies (squares) and the conduction network (lines) for $\text{Na } \beta''\text{-alumina}$. (a) Perfect vacancy superlattice, (b) a single vacancy, (c) superlattice with a vacancy-depleted region, and (d) superlattice with a vacancy-excess region. The dashed lines in (c) and (d) indicate the potential well each vacancy sits in.

high temperatures (~ 0.03 eV at 750 K) determined from the conductivity data (Fig. 2). Otherwise, if the activation energy for a single vacancy to jump were high, then it would be very difficult to explain why the activation enthalpy can be so low at some temperatures and is so sensitive to the temperature change. For our present case, we can argue that because a single vacancy is nearly free, then when many vacancies are present in the crystal, they can rearrange their positions according to their mutual interaction very easily. When the concentration is right, a superlattice may even be formed. Figures 3 and 4(a) show schematically such a superlattice for $\text{Na } \beta''\text{-alumina}$ according to the diffuse x-ray scattering result.⁸ It is conceivable that the ordering of vacancies around a given vacancy will add extra restraint to its motion. The high value of ΔH below 350 K in Fig. 2 may, therefore, be attributed to such a vacancy ordering on the superlattice at low temperatures.

B. Vacancy ordering and $\Delta H(T)$

To construct a conduction model for $\text{Na } \beta''\text{-alumina}$ and to understand the connection between the temperature dependence of ΔH shown in Fig. 2 and the ordering of vacancies, we first assume that at $T=0$ the vacancies form a perfect superlattice as shown in Fig. 4(a). Because of the ordering of other vacancies, each vacancy is restrained to its regular superlattice site. However, at finite temperatures, because of thermal agitations, some of the vacancies are excited out of their superlattice sites to form "Frenkel defects." This is demonstrated in Figs. 4(c) and 4(d): A vacancy at o in Fig. 4(c) is excited to another region near o in Fig. 4(d). As a result, regions of missing and extra vacancies are formed.

We can argue that the ionic conduction is mainly due to these "Frenkel defects" and $\Delta G(T)$ in Eq. (5) consists of two parts²⁰: that due to the formation of the Frenkel defects, $\Delta G_F(T)$, and that due to the motion of the defect (disordered vacancies), $\Delta G_M(T)$, i.e.,

$$\Delta G(T) = \Delta G_F(T)/2 + \Delta G_M(T). \quad (10)$$

The factor $\frac{1}{2}$ in Eq. (10) originates from the configurational entropy and from the result that the concentration of Frenkel defects n_F is related to the total concentration n of the superlattice sites [which is equal to the total vacancy concentration in Fig. 4(a)] by²¹

$$n_F = n \exp[-\Delta G_F(T)/2kT]. \quad (11)$$

Similarly, $\Delta H(T)$ in Eqs. (2) and (5) also consists of two parts:

$$\Delta H(T) = \Delta H_F(T)/2 + \Delta H_M(T). \quad (12)$$

It is conceivable that the part of the activation enthalpy due to defect motion, $\Delta H_M(T)$, is small and comparable to that of a single vacancy [Fig. 4(b)]. This is because a vacancy excited out of its superlattice site will no longer receive the extra restraint due to the ordering of other vacancies on the superlattice. The formation enthalpy $\Delta H_F(T)$ is expected to depend on the extent of the vacancy ordering on the superlattice. When the vacancies are completely disordered, $\Delta H_F(T)$ is expected to be zero.

The temperature dependence of ΔH shown in Fig. 2 can now be interpreted in the following way: According to diffuse x-ray measurements for Na β'' -alumina,^{7,8} the extent of vacancy ordering on the superlattice is temperature dependent; the coherence length (the size of the ordered region), $\xi(T)$, is about 70 Å below 300 K and decreases with increasing temperature to about 20 Å at 600 K. It is likely that the decrease in ΔH with increasing temperature is mainly due to the reduction of the formation enthalpy $\Delta H_F(T)$ which, in turn, is mainly determined by $\xi(T)$. At high temperatures, when the ordering of vacancies is almost completely destroyed, $\Delta H(T)$ is reduced to that for a nearly free single vacancy (~ 0.02 eV).

To understand qualitatively the connection between ΔH and ξ , we assume that the vacancies within a circle of radius ξ about the superlattice site o [Figs. 4(c) and 4(d)] are ordered and those outside the circle are completely random. The Coulomb energy needed to create a vacancy-depleted region [Fig. 4(c)] and a vacancy-excess region [Fig. 4(d)], ΔE_F , due to the ordered vacancies is of the form

$$\Delta E_F \approx 2 \left[\sum_{r'_i < \xi} e^2/\epsilon r'_i - \sum_{r_i < \xi} e^2/\epsilon r_i \right], \quad (13)$$

where ϵ is the dielectric constant, r_i is the distance between site o and the vacancy i , and r'_i is the dis-

$$\Delta E_F \approx \text{const} + \frac{2e\rho}{\epsilon} \int_{r_0}^{\xi} \int_0^{2\pi} \left[\frac{1}{(r^2 + z^2 - 2zr \sin\theta)^{1/2}} - \frac{1}{r} \right] r dr d\theta, \quad (15)$$

where z is the distance between position o and one of the two vacancies next to it in Fig. 4(d). By assuming that r_0 and ξ are much greater than z , the integral in Eq. (15) can be evaluated. The result up to the z^2 term is given by

$$\Delta E_F \approx \text{const} - \pi e \rho z^2 / \epsilon \xi. \quad (16)$$

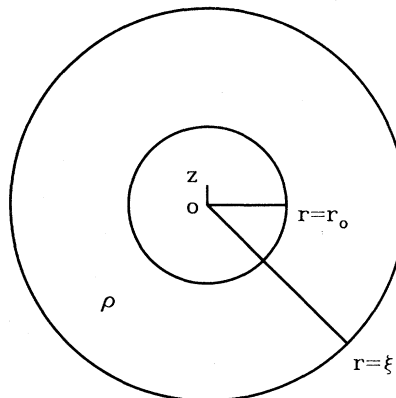


FIG. 5. Annular two-dimensional charge distribution with charge density ρ used in the evaluation of the integral in Eq. (15). The line oz corresponds to the separation between the position o and one of the closest vacancies in Fig. 4(d). Vacancies within $r = \xi$ are assumed to be completely ordered.

tance between the vacancy i and one of the two vacancies surrounded by the dashed lines in Fig. 4(d). The factor 2 in Eq. (13) comes from the fact that to create a Frenkel defect shown in Figs. 4(c) and 4(d), the two vacancies on positions o in the figures are removed and the two vacancies next to position o in Fig. 4(d) are added. To evaluate the summations in Eq. (13), we first write

$$\Delta E_F \approx \text{const} + 2 \left[\sum_{r_0 < r'_i < \xi} e^2/\epsilon r'_i - \sum_{r_0 < r_i < \xi} e^2/\epsilon r_i \right], \quad (14)$$

where r_0 is some radius greater than the superlattice parameter a' . By doing so, the contribution to ΔE_F from the vacancies within radius r_0 in Eq. (13) is absorbed into the constant in Eq. (14). We next approximate the ordered vacancies in the annular region $r_0 < r < \xi$ with a uniform two-dimensional charge distribution with charge density ρ (Fig. 5). The summations in Eq. (14) can then be converted to an integral:

The main contributions to ΔH and ΔH_F are the changes in potential energies; the contributions from the volume changes $P\Delta V$ are negligibly small (e.g., for $P=1$ atm and $\Delta V \approx$ volume of an atom $\approx 30 \text{ \AA}^3$, $P\Delta V = 1.9 \times 10^{-5}$ eV). If we assume that the ξ dependence of ΔH and ΔH_F is mainly

through ΔE_F , then the activation enthalpy can be written in the form

$$\Delta H(T) = a - b/\xi(T), \quad (17)$$

where a and b are constants.

A least-squares fit of the calculated $\Delta H(T)$ with Eq. (17) using the experimental $\xi(T)$ reported in Ref. 8 is shown in Fig. 2. (For this fit the values of a and b were found to be 0.454 eV and 7.17 eV/Å, respectively.) It can be seen from the figure that the fit is quite good, suggesting that there is a strong correlation between the temperature dependence of the activation enthalpy ΔH and the ordering of the vacancies on the superlattice. Notice that in deriving Eq. (17), the two-dimensional nature of the problem was used in writing Eq. (13).

C. Temperature dependence of ΔS and ΔG

As can be seen from Eqs. (3) and (5), a temperature-dependent ΔH implies a temperature-dependent ΔS and ΔG . In calculating $\Delta S(T)$ with Eq. (9), the integration constant ΔS_0 was set to be zero, which is equivalent to setting $\Delta S=0$ at $T=\infty$. Here we present some justifications. From Eqs. (5), (10), and (12), one has

$$\Delta S(T) = \Delta S_F(T)/2 + \Delta S_M(T), \quad (18)$$

where $\Delta S_F(T)$ is the formation entropy for a Frenkel defect and $\Delta S_M(T)$ is the activation entropy for defect motion. At very high temperatures, all vacancies become random. This implies that $\Delta G_F = \Delta H_F = \Delta S_F = 0$ and $\Delta S = \Delta S_M$ at $T = \infty$. We next show that $\Delta S_M = 0$ at $T = \infty$ will yield a reasonable value of ν_0 which appears in Eqs. (2) and (4). This is done by first finding the constant C in these equations at high temperatures.

To find the constant C , we note that σ and the diffusion coefficient D_V of the vacancies are related by the Nernst-Einstein relation

$$\sigma T = ne^2 D_V / k, \quad (19)$$

where n , as defined in Eq. (11), is the vacancy density and e is the electron charge. From the two-dimensional random-walk theory one has

$$D_V = vd^2/4, \quad (20)$$

where d is the jump distance and is equal to $a/\sqrt{3}$, and v is the jump frequency which can be written as²²

$$v = s(1 - n/N)\nu_0 \exp[-\Delta G(T)/kT]. \quad (21)$$

In Eq. (21), s is the number of equivalent paths of diffusion from a given site, n/N is the fraction of vacant sites, and ν_0 is the attempt frequency for a vacancy to jump to a given occupied neighboring site. For Na β'' -alumina^{8,16} $1 - n/N \approx \frac{5}{6}$ and at high temperatures, $s=3$. Therefore, from Eqs. (4), (19), (20), and (21) one has

$$C = n(1 - n/N)e^2 a^2 / 4k. \quad (22)$$

The vacancy density can be calculated from the lattice parameters^{8,16} $a = 5.623$ Å and $c = 33.591$ Å for Na β'' -alumina to be $n = 1.09 \times 10^{21}$ cm⁻³. Equation (4) can then be written as

$$\sigma T = 39.9\nu_0 \exp\{-[\Delta H(T) - T\Delta S(T)]/kT\}, \quad (23)$$

where σT is in units of (Ω cm)⁻¹ K and ν_0 is in cm⁻¹. With the use of $\Delta H(T)$ and $\Delta S(T)$ in Fig. 2 and the conductivity data for Na β'' -alumina in Fig. 1, the value of ν_0 was determined to be 32.2 cm⁻¹, which is consistent with the Raman band near 30 cm⁻¹ assigned^{18,23} as the attempt mode for Na⁺ ion diffusion in β'' -alumina.

The temperature dependence of ΔG is determined by ΔH and ΔS through Eq. (5). Because of the large value of ΔS , ΔG is much smaller than ΔH at low temperatures (Fig. 2).

V. SUMMARY

As shown by Eq. (7), the experimental heat of activation obtained from the slope of the Arrhenius plot, $\log(\sigma T)$ vs $1/T$, is identical to the activation enthalpy ΔH if we assume that only one conduction mechanism is involved. The activation enthalpy calculated for the Na β'' -alumina conductivity data analyzed in this work has a high constant value of about 0.33 eV below 350 K and decreases with increasing temperature to about 0.03 eV at 750 K. This temperature dependence can be understood by analyzing the ordering of the Na⁺ ion vacancies on a superlattice. As can be seen from Fig. 2, the activation enthalpy and the extent of the vacancy ordering, described by the coherence length ξ , can be correlated quite well with the form shown by Eq. (17). In this respect, the small calculated activation energy for a single vacancy in the ideal structure shown in Fig. 4(b) is consistent with the fact that ΔH can be very small at some temperatures and is very sensitive to temperature changes.

The temperature dependence of ΔS and ΔG shown in Fig. 2 is a natural result of the tempera-

ture dependence of ΔH through Eqs. (3) and (5). The value of ΔS decreases with increasing temperature from a high value of about $7k$ (10^{-22} J/K) below 300 K to about 0 at 750 K. As a result, the activation free energy in Eq. (4) determined from $\Delta G(T) = \Delta H(T) - T\Delta S(T)$ is much lower than the apparent activation energy, which is identical to $\Delta H(T)$, determined from Eq. (6) at low temperatures.

ACKNOWLEDGMENTS

The author wishes to thank J. B. Bates, N. J. Dudney, H. Engstrom, S. H. Liu, D. F. Pickett, Jr., and H. Sato for helpful discussions. This work was sponsored by the Division of Materials Sciences, U.S. Department of Energy under Contract No. W-7405-eng-26 with Union Carbide Corporation.

APPENDIX

It was shown¹⁵ that if a $\log(\sigma T)$ vs $1/T$ plot is continuous and smooth, then σT can always be written as

$$\sigma T = \nu_0 C \exp\{-[\Delta H(T) - T\Delta S(T)]/kT\}, \quad (\text{A1})$$

where the product $\nu_0 C$ is a constant and the func-

tions $\Delta H(T)$ and $\Delta S(T)$ satisfy the relation

$$\frac{d\Delta H(T)}{dT} = \frac{Td\Delta S(T)}{dT}. \quad (\text{A2})$$

Here we outline a similar but slightly different derivation of the result. Let X denote $1/kT$. From the assumption we can write

$$\ln(\sigma T/\nu_0 C) = Y(X), \quad (\text{A3})$$

where $Y(X)$ is a continuous and smooth function of X . Let $P(X)$ be the slope of $Y(X)$ at X , i.e.,

$$P(X) = \frac{dY(X)}{dX}, \quad (\text{A4})$$

and $I(X)$ be the intercept of the tangent of $Y(X)$ at X with the Y axis. From analytic geometry one has

$$Y(X) = XP(X) + I(X). \quad (\text{A5})$$

From Eqs. (A3) and (A5) one gets

$$\sigma T = \nu_0 C \exp[XP(X) + I(X)]. \quad (\text{A6})$$

By differentiating Eq. (A5) and using Eq. (A4) one gets

$$\frac{dI(X)}{dX} = -X \frac{dP(X)}{dX}. \quad (\text{A7})$$

If now we define $-P(X) \equiv \Delta H(T)$ and $kI(X) \equiv \Delta S(T)$, then Eqs. (A6) and (A7) become identical to Eqs. (A1) and (A2), respectively.

- ¹M. Bettman and C. R. Peters, *J. Phys. Chem.* **73**, 1774 (1969).
- ²J. T. Kummer, *Prog. Solid State Chem.* **7**, 141 (1972).
- ³T. Cole, N. Weber, and T. K. Hunt, in *Fast Ion Transport in Solids, Electrodes and Electrolytes*, edited by P. Vashishta, J. N. Mundy, and G. K. Shenoy (North-Holland, New York, 1979), p. 277.
- ⁴G. C. Farrington and J. L. Briant, in *Fast Ion Transport in Solids, Electrodes and Electrolytes*, Ref. 3, p. 395.
- ⁵J. L. Briant and G. C. Farrington, *J. Solid State Chem.* **33**, 385 (1980).
- ⁶H. Engstrom, J. B. Bates, W. E. Brundage, and J. C. Wang, *Solid State Ionics* **2**, 265 (1981).
- ⁷G. Collin, Ph. Colombar, J. P. Boilot, and R. Comes, in *Fast Ion Transport in Solids, Electrodes and Electrolytes*, Ref. 3, p. 309.
- ⁸J. P. Boilot, G. Collin, Ph. Colombar, and R. Comes, *Phys. Rev. B* **22**, 5912 (1980).
- ⁹J. C. Wang, J. B. Bates, N. J. Dudney, and H. Engstrom, *Solid State Ionics* **5**, 35 (1981).
- ¹⁰J. B. Bates, H. Engstrom, J. C. Wang, B. C. Larson, N.

- J. Dudney, and W. E. Brundage, *Solid State Ionics* **5**, 159 (1981).
- ¹¹H. Sato and R. Kikuchi, *J. Chem. Phys.* **55**, 677 (1971).
- ¹²R. Kikuchi and H. Sato, *J. Chem. Phys.* **55**, 702 (1971).
- ¹³J. C. Wang, in *Electrochemical Society Extended Abstracts* (Electrochemical Society, Pennington, New Jersey, 1982), Vol. 82-1, p. 1147.
- ¹⁴J. B. Bates, J. C. Wang, and N. J. Dudney, *Phys. Today* **35** (7), 46 (1982).
- ¹⁵G. B. Gibbs, *Acta Metallurg.* **15**, 1551 (1967).
- ¹⁶W. L. Roth and S. LaPlaca (private communication).
- ¹⁷J. C. Wang, J. B. Bates, T. Kaneda, and H. Engstrom, *Bull. Am. Phys. Soc.* **24**, 433 (1979).
- ¹⁸J. B. Bates, G. M. Brown, T. Kaneda, W. E. Brundage, J. C. Wang, and H. Engstrom, in *Fast Ion Transport in Solids, Electrodes and Electrolytes*, Ref. 3, p. 261.
- ¹⁹J. C. Wang and D. F. Pickett, Jr., *J. Chem. Phys.* **65**, 5378 (1976).
- ²⁰J. R. Manning, in *Diffusion Kinetics for Atoms in Cryst-*

- tals* (Van Nostrand, Toronto, 1968), p. 12.
- ²¹C. Kittel, in *Introduction to Solid State Physics*, 3rd ed. (Wiley, New York, 1967), p. 570.
- ²²C. A. Wert, *Phys. Rev.* 79, 601 (1950).
- ²³J. B. Bates, T. Kaneda, W. E. Brundage, J. C. Wang, and H. Engstrom, *Solid State Commun.* 32, 261 (1979).